Hindawi
Advances in Civil Engineering
Volume 2019, Article ID 8752465, 16 pages
https://doi.org/10.1155/2019/8752465

Research Article

Seismic Failure Pattern Prediction in a Historical Masonry Minaret under Different Earthquakes

Halil Nohutcu

Manisa Celal Bayar University, Engineering Faculty, Civil Engineering Department, 45140 Manisa, Turkey

Correspondence should be addressed to Halil Nohutcu; halil.nohutcu@cbu.edu.tr

Received 1 October 2018; Accepted 25 November 2018; Published 22 January 2019

Academic Editor: Humberto Varum

Historical structures are the values that are of great importance to that country, showing the roots of a country, and must be passed on from generation to generation. This study attempts to make a contribution to this goal. Seismic damage pattern estimation in a historical brick masonry minaret under different ground motion levels is investigated by using updated finite element models based on ambient vibration data in this study. Imaret Mosque which was built in 1481 AD is selected for an application. Surveying measurement and material tests were conducted to obtain a 3D solid model and mechanical properties of the components of the minaret. Firstly, the initial 3D finite element model of the minaret was analyzed and numerical dynamic characteristics of the minaret were obtained. Then, ambient vibration tests as well as operational modal analysis were implemented in order to obtain the experimental dynamic characteristics of the minaret. The initial finite element model of the minaret was updated by using the experimental dynamic results. Lastly, linear and nonlinear time-history analyses of the updated finite element model of the minaret were carried out using the acceleration records of two different level earthquakes that occurred in Turkey, in Afyon-Dinar (1995) and Çay-Sultandağı (2002). A concrete damage plasticity model is considered in the nonlinear analyses. The conducted analyses indicate that the compressive and tension stress results of the linear analyses are not as realistic as the nonlinear analysis results. According to the nonlinear analysis, the Çay-Sultandağı earthquake would inflict limited damage on the minaret, whereas the Dinar earthquake would damage some parts of the elements in the transition segment of the minaret.

1. Introduction

Architectural and structural characteristics of minarets are influenced by national and local building materials. Historical minarets are generally masonry structures in which stone or clay brick and mortar are used together. The behavior of the majority of historical structures differs from one another during an earthquake as local materials are used in their construction. There is usually a spiral staircase system made of wood or stone inside the minarets. The most important feature of historical masonry structures is that they reflect the architectural characteristics of the time at and the region in which they were built [1]. For example, in the thirteenth-century Syrian architecture, minarets were built as low square towers sitting at the four corners of the mosque. In the fifteenth-century Egyptian architecture, minarets were octagonal and had two balconies, the upper generally smaller than the lower. Turkish-style minarets were slim and consisted of 2, 4, or 6 circular minarets of equal cross section [2]. Minarets generally consist of 8 parts: a base (footing), cube (pulpit), transition segment, shaft (cylindrical or polygonal), balcony, comb, cone (spire), and finial. The height and shaft diameter of minarets vary from 10 to 40 m and 3 to 6 m, respectively.

Many tower-type masonry structures were completely or partially destroyed due to major earthquakes, strong winds, or suddenly without any indication. For example, the Yüregil Minaret in Afyonkarahisar and the Çavdır Minaret in Antalya, Turkey, are some of the structures that were damaged in earthquakes, whereas the Civic Tower in Pavia in Italy collapsed without any indication [3]. These dramatic events have obligated determining the behavior of tower-type structures under wind and earthquake conditions so that they may be safely passed on to the next generations. For

this reason, the protection and the evaluation of the structural safety of historic masonry structures have become compulsory. Ambient vibration testing and finite element methods are promising techniques for safety and damage evaluation of the masonry structures [4, 5]. The studies on the analytical and experimental behaviors of masonry towers and minarets can be found in the literature. Gentile et al. determined the structural safety of tower of the Monza Church using ambient vibration data and updated the finite element model of the tower [6]. Pallarés et al. carried out a nonlinear analysis of a chimney made of bricks using the Drucker–Prager material model [7]. Bayraktar et al. investigated the earthquake behavior of İskenderpaşa Mosque Minaret in Trabzon, Turkey, and reported that cracks due to earthquake can occur at the region between the transition segment and the cylindrical body [5]. Tomaszewska and Szymczak identified the Vistula Mounting Tower model using measured modal data [8]. Foti et al. determined the structural condition of a tower in Bari, Italy, and obtained an excellent match between the experimental and the updated model results [9]. Mortezaei et al. investigated linear and nonlinear earthquake behaviors of the masonry Masjed-e-Jame Mosque and minaret in Iran. Researchers have also revealed the effect of strengthening on the structures [10]. D'Ambrisi et al. updated the finite element model of the Civic Tower in Italy by operational modal analysis (OMA) and revealed the nonlinear seismic performance of the tower [11]. Bartoli et al. implemented static and dynamic investigations on the stone tower Torre Grossa [12]. Minghini et al. conducted a study on a brick masonry chimney damaged during the Emilia earthquake in 2012 [13]. Diaferio et al. determined the nondestructive characterization and identification of the modal parameters of an old masonry tower [14]. Diaferio et al. extracted the natural frequencies and mode shapes of the bell tower of Trani's Cathedral in Italy via conventional accelerometers and innovative microwave remote sensing to operational modal testing [15]. The frequency-domain decomposition (FDD)/enhanced frequency-domain decomposition (EFDD) and the data-driven stochastic subspace identification (SSI) techniques have been used for the extraction of modal parameters. The authors revealed that the results obtained by the two measurement systems are in good agreement and encourage the effectiveness of the tests and the accuracy of the estimated modal parameters. Diaferio et al. investigated a slender historical bell tower in Bari to obtain the accurate finite element model [15]. Despite the impossibility of conducting destructive tests to evaluate the material properties, by conducting environmental vibration tests and comparing first five modes, they achieved to obtain the accurate finite element model (FEM). Preciado suggested a procedure for the seismic vulnerability evaluation of all types of towers and slender masonry structures such as light houses and minarets [16]. Preciado et al. proposed an approach for the seismic vulnerability reduction of masonry towers via external prestressing devices [17]. Hejazi et al. investigated the response of nine minarets under different temperatures, wind, and earthquakes using a nonlinear finite element model. In the study, they have revealed that earthquakes are the main cause of collapse of the minarets [18]. Demir et al. investigated the effect of model calibration on seismic behavior of the structure [19]. Maximum stresses and displacements in the structure were presented comparatively. Also, locations of existing cracks in the structure coincided with the analysis results. Livaoğlu et al. investigated Ottoman-type minarets and obtained a numerical correlation between the first mode period and geometric properties, such as height, cross section, and boundary conditions via operational modal analysis [20]. Kocaturk and Erdogan modelled minarets via a commercial finite element method (FEM) program, ANSYS/LS-DYNA, and revealed the contribution of lead clamps to the energy absorption capacity of the minaret under extensive earthquakes [21]. Ivorra et al. conducted a theoretical dynamic study on a masonry bell tower and investigated the correlation between natural frequencies and variation of soil [22]. Shakya et al. collected the data from various literature on the slender masonry structures and developed an empirical formulation for predicting the fundamental frequency of such structures [23]. Diaferio et al. performed operational modal analysis of the bell tower of Announziata in order to obtain the updated FE model of the tower [15]. Castellazzi et al. monitored the San Pietro bell tower in Perugia, Italy, for 9 months, and the effects of changes in temperature and humidity on the natural frequencies of slender masonry buildings are investigated by using environmental vibrations [24]. Diaferio and others have experimentally investigated a historic stone masonry building with OMA under environmental vibration and emphasized the need for improvement of the finite element model for realistic analysis [25].

In general, model updating techniques are based on the use of appropriate coefficients (sensitivity coefficients) that iteratively update selected physical properties (properties of materials, stiffness of a link, etc.) in such a way that the correlation between the simulated response and the target value could improve if compared to an initial value [26]. This study is aimed at estimating seismic damage propagation in a historical clay brick masonry minaret under different ground motion levels by using the updated finite element model based on ambient vibration data. Imaret Mosque Minaret in the county of Bolvadin in Afyon, Turkey, was selected for the application. Material properties of the minaret were determined by the material tests. Experimental dynamic characteristics of the minaret were obtained by ambient vibration testing. The experimental dynamic characteristics were compared with the numerical dynamic characteristics obtained from initial three-dimensional FEM of the minaret, and the initial model was updated by changing the material properties and boundary conditions. Linear and nonlinear time-history analyses of the updated FEM of the minaret were carried out using the acceleration records of two different level earthquakes that occurred in Turkey, in Afyon-Dinar (1995) and Çay-Sultandağı (2002). Nonlinear analysis was performed using the concrete damage plasticity (CDP) model [27]. The damage of the historical minaret against the two selected earthquakes was obtained, and it was determined that the minaret was at risk of collapse during a severe earthquake.

2. Materials and Methods

2.1. Geometric and Mechanical Properties of Imaret Minaret. Bolvadin is one of the oldest settlements in Anatolia. It dates back to 10,000 years ago according to available documentation (Bayar, 1996). Especially during the reign of the Seljuks, it was decorated with mosques, fountains, inns, baths, aqueducts, and bridges. The Imaret Mosque, built in 1481 AD, is one of these works that has survived to the present day. The bearing system of the minaret consists of clay brick except pulpit which is stone masonry. The height of the minaret is 24.5 m, the pulpit has 2.66 × 2.66 m octagonal section, and the cylindrical body has a diameter of 2.0 m. Parts of the minaret and vertical and horizontal cross sections of the minaret are presented in Figure 1.

2.2. Material Properties. The material properties of the minaret are taken from the similar study of Nohutcu et al. and are listed in Table 1 [28].

The minaret consists of stone/brick and mortar materials. Elastic material parameters of the masonry wall using materials test results were calculated by equations recognized in the literature. The compressive strength of masonry is determined by equation (1) from the European Committee for Standardization (1995, p. 51) [29]. Here, K values vary from 0.4 to 0.6 with a difference of 0.5 according to the morphological structure of the masonry system. The values of α and β are 0.7 and 0.3, respectively, in smooth-shaped masonry and 0.65 and 0.25 in coarse-shaped masonry, respectively. f_b (MPa) refers to the compressive strength of the stone or brick. f_m (MPa) is the compressive strength of the mortar and is the maximum value that can be taken as double the value of f_b:

$$f_k = K \cdot f_b^{\alpha} \cdot f_m^{\beta}. \quad (1)$$

The modulus of elasticity of masonry is determined using equation (2) derived by Lourenco in 2001 [30]. The tensile strength is taken as 10% of the compressive strength. Poisson's ratio is recommended as 0.17 by Koçak [31]. In equation (1), ρ is a fixed value and varies according to the adherence between mortar and stone/brick. t_m refers to the average thickness of the mortar, t_u is the average height of the stone or brick, E_m is the modulus of elasticity of the mortar, and E_u is the modulus of elasticity of the stone or brick [30]:

$$E = \frac{t_m + t_u}{(t_m/E_m) + (t_u/E_u)}\rho. \quad (2)$$

Table 2 presents the calculated material parameters of the masonry walls, used in the finite element analyses of the minaret.

2.3. Initial Finite Element Model of the Minaret. According to the drawings obtained from in situ surveying measurements, the three-dimensional solid model and FEM model of the minaret were prepared using the Abaqus [27] software (Figure 2). Convergence analysis was conducted for the purpose of determining the most appropriate range of mesh in the FEM of the minaret. In the convergence analysis, the mesh size was initially selected as 0.55 m. Modal analyses were carried out for each range of the mesh given in Table 3, and the convergence graphics is given in Figure 3.

According to the convergence analysis values in Table 3, the range of the mesh in numerical analysis was chosen as 0.25 m. A total of 28175 four-node tetrahedral (C3D4) solid elements and 8646 nodes were used for the initial FEM with a mesh size of 0.25 m. The modal analysis was carried out, and the first four numerical frequency values and mode shapes profile and plan views are presented in Figure 4. The first and the third mode shapes occur in the x direction, and the second and the fourth mode shapes occur in the y direction.

2.4. Operational Modal Analysis and Finite Element Model Updating of the Minaret. The material values are the local properties of the wall material. When we apply these values to the whole structure, it is difficult to achieve realistic values due to the regional differentiations. Therefore, operational modal analysis is performed with the data obtained from the accelerometers, which takes the environmental vibration data on the structure. Thus, experimental modal behavior and damping rates of the structure can be obtained. By modifying the modulus of elasticity, a modal analysis is carried out by the finite element method until it reaches the modes we have found experimentally. When we reach the first mode value obtained from OMA, we obtain the modulus of elasticity and the damping ratio of the structure.

Four Testbox-2010 data acquisition devices and sixteen uniaxial Sensebox-7021 accelerometers were used for the OMA method. The accelerometers used in the experiment are sensitive to signals in the range 0–200 Hz. The signals from the accelerometers are combined in the four-channel Testbox-2010 data acquisition unit and transferred to the Testlab-Network [32] data acquisition software. After the signals were processed, experimental dynamic characteristics of the structure were obtained by using the ARTeMIS Modal Pro [33] software.

OMA is an output-only method based on ambient vibration data. In the experimental study, the connection points of the accelerometers were identified using the initial finite element (FE) mode shapes of the minaret. A total of 12 uniaxial accelerometers were placed at these points as shown in Figure 5. Vibrations generated by the environmental effects on the minaret were collected by 12 uniaxial accelerometers and data acquisition units.

Acceleration data obtained from the OMA test were transferred to the ARTeMIS Modal Pro [33] software, and the experimental dynamic parameters of the minaret were extracted using the SSI technique [34, 35]. The stabilization diagram of estimated state space models obtained from the SSI technique and the experimental dynamic characteristics are given in Figure 6 and Table 4, respectively.

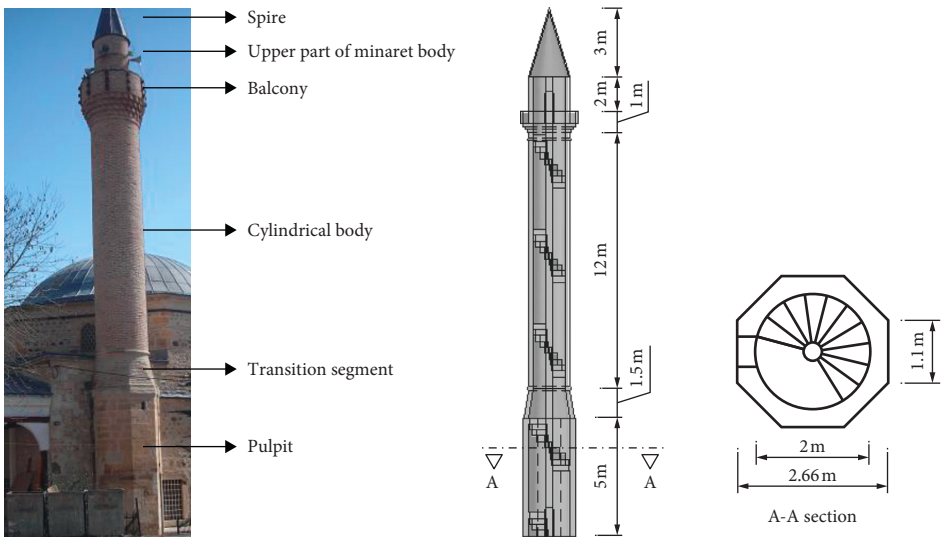

Figure 1: (a) Parts of the minaret. (b) Vertical and horizontal cross sections of the minaret.

Table 1: Stone and brick material parameters from another similar study [28].

	Compressive strength (MPa)	Tensile strength (MPa)	Modulus of elasticity (MPa)	Ultrasonic pulse velocity (m/s)	Surface hardness (R)	Density (kg/m^3)
Andesite stone	30	2.08	12240	1813	54	2200
Full brick	8.2	1.86	2985	1051	31	2100
Khorasan mortar	6.25	1.43	1100	—	—	1340

Table 2: Initial material parameters of masonry walls.

Materials	Stone masonry	Brick masonry
Compressive strength (MPa)	7.210	4.210
Tensile strength (MPa)	0.721	0.421
Modulus of elasticity (MPa)	4400	1300
Bulk density (kg/m^3)	2200	1750
Poisson's ratio	0.17	0.17

It can be seen from Table 4 that there are differences between the numerical and experimental frequencies. The updated FEM of the minaret is obtained by changing Young's modulus of brick. Modulus of elasticity of the brick masonry wall increases from 1300 MPa to 5200 MPa. Table 5 presents the first four numerical and experimental frequency values obtained before and after the model calibration of the minaret. The four mode shapes were obtained from the tests as shown in Figure 7(b). It can be seen from Table 5 and Figure 7 that the calibrated and experimental frequencies and mode shapes are close to each other. Besides, it can be seen from Figures 4 and 7 that the two mode shapes obtained from the initial and calibrated FEM occur in the same directions.

2.5. Seismic Damage Pattern Estimation of the Minaret. Seismic damage propagation in the minaret was determined by means of linear and nonlinear finite element models in

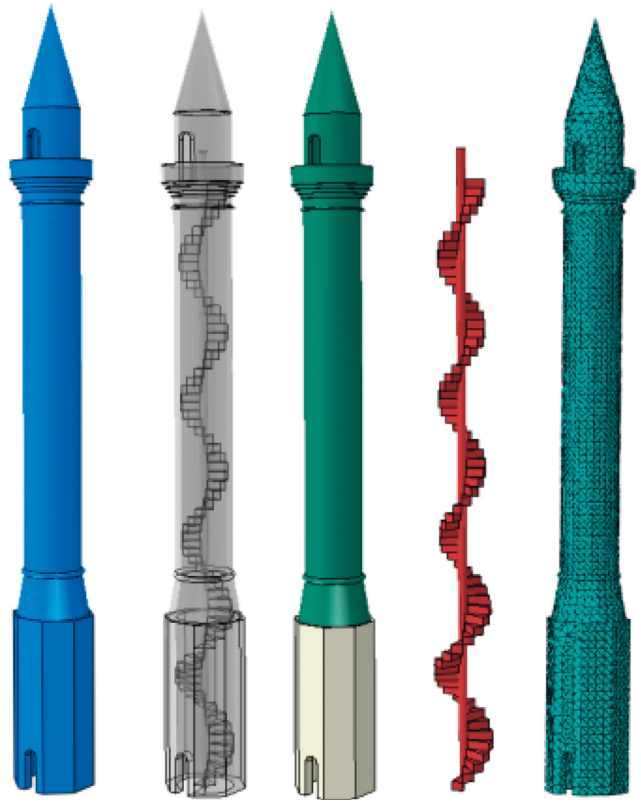

Figure 2: Three-dimensional solid model and finite element model of the minaret.

Table 3: Mesh size convergence.

Mesh size (m)	The first frequency (Hz)	Number of elements
0.55	0.896	8710
0.50	0.869	9546
0.45	0.863	11170
0.35	0.854	17404
0.25	0.849	28175
0.15	0.846	105985

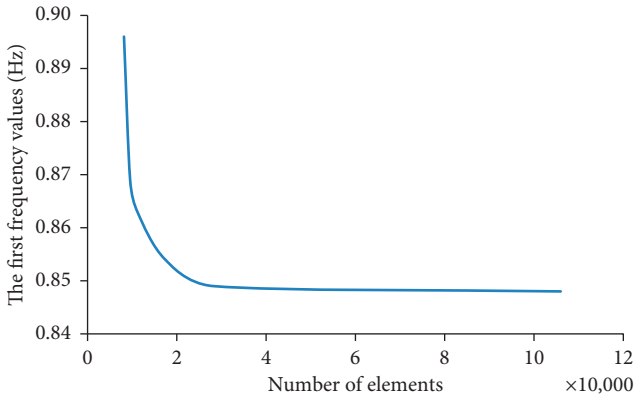

Figure 3: Frequency and mesh size convergence graphic.

Abaqus. The nonlinear analyses were performed using the CDP model. The CDP model depends on the integration of damage mechanics, and plasticity is improved to analyze the failure of concrete and unreinforced brittle masonry structures. CDP describes the important characteristics of the failure process of concrete or masonry under multiaxial stress. Material parameters for masonry in the CDP model are summarized in Table 6.

The failure of masonry can be modelled under uniaxial compression and tension and by the plasticity characteristics. CDP model response under uniaxial compression and tension is linear until the initial value of yield stress. When the failure stress is reached, microcrack formation in masonry is activated. In the plastic regime, the response is typically characterized by stress hardening followed by strain softening. Beyond the failure stress, the formation of microcracks is represented macroscopically with a softening stress-strain response as shown in Figure 8.

Material properties of the masonry used in the minaret were adopted from the study carried out by Kaushik et al. [36] and are shown in Figure 9.

The acceleration records of the earthquakes that took place in Çay-Sultandağı (Mw 6.0) on Feb 3, 2002, and Dinar (Mw 6.0) on Oct 10, 1995, were used to determine the seismic damage patterns of Imaret Mosque Minaret. Time histories of two components of the earthquakes are depicted in Figure 10. The records are applied to the minaret in x-x and y-y horizontal directions simultaneously.

2.6. Linear Analysis of Minaret under Çay-Sultandağı and Dinar Earthquakes. Linear time-history analyses of the minaret are performed using the full Newton method in Abaqus [27]. The damping ratio is chosen as 5%. The maximum lateral displacement values in $U1$ (x) and $U2$ (y) directions are 4.4 cm and 5.3 cm under the Çay-Sultandağı earthquake and 12.9 cm and 37.6 cm under the Dinar earthquake, respectively (Figure 11). The lateral displacement values throughout the height of the minaret under linear analysis for Çay-Sultandağı and Dinar earthquakes are presented in Figure 12.

Under the Çay-Sultandağı earthquake, it was observed that the maximum (tension) principal stress (126 MPa) was concentrated around the door which is in the transition segment that lies between the pulpit and the cylindrical body, while the minimum (compression) principal stress (1.36 MPa) was concentrated on the opposite side of the door (Figure 13). Under the Dinar earthquake, the maximum and minimum principal stresses occurred in the same location and were obtained as 7.7 MPa and 8.1 MPa, respectively, as shown in Figure 14. The maximum and minimum stresses that occurred in the minaret under the Dinar earthquake exceeded limit tension (0.421 MPa) and compression (4.21 MPa) values of the masonry wall. However, in the Çay-Sultandağı earthquake, only maximum principal stresses slightly exceeded tensile stresses (0.421 MPa) of the wall material. Therefore, it was shown that Çay-Sultandağı does not cause a serious damage to the minaret. During the Dinar earthquake, maximum tensile and compressive stresses exceeded the limit tensile stress about 6 and 19 times, respectively. So, linear analysis has shown that the minaret could damage substantially under the Dinar earthquake impact.

2.7. Nonlinear Analysis of Minaret under Çay-Sultandağı and Dinar Earthquakes

2.7.1. Çay-Sultandağı Earthquake. According to the results of nonlinear time-history analysis for the Çay-Sultandağı earthquake, the maximum lateral displacement values are obtained as 4.8 cm and 3.6 cm in $U1$ and $U2$ directions, respectively (Figure 14). Critical maximum and minimum principle stress contours under the Çay-Sultandağı earthquake are presented in Figure 15.

In CDP analysis, the damage of the minaret can be achieved. When this damage ratio exceeds 100 percent, it is accepted that the structure completely collapsed. When the plastic deformation obtained with the nonlinear solution is investigated, it was found that the safety boundary deformation values also exceeded. But the main criterion that determines the damage and destruction of the structure is the damage rate obtained by the CDP.

The damage effect compression stress on the minaret is calculated by CDP analysis, and the damage percentage contours at the end of time steps are presented in Figure 16.

The compression damage on masonry of the minaret begins at 11.73 s, and the plastic deformation value reaches 0.0057 at the end of the analysis (t = 25 s) (Figure 17). Limited number of elements exceeds the value of 0.004 which is the critical damage strain value of the masonry (Figure 9).

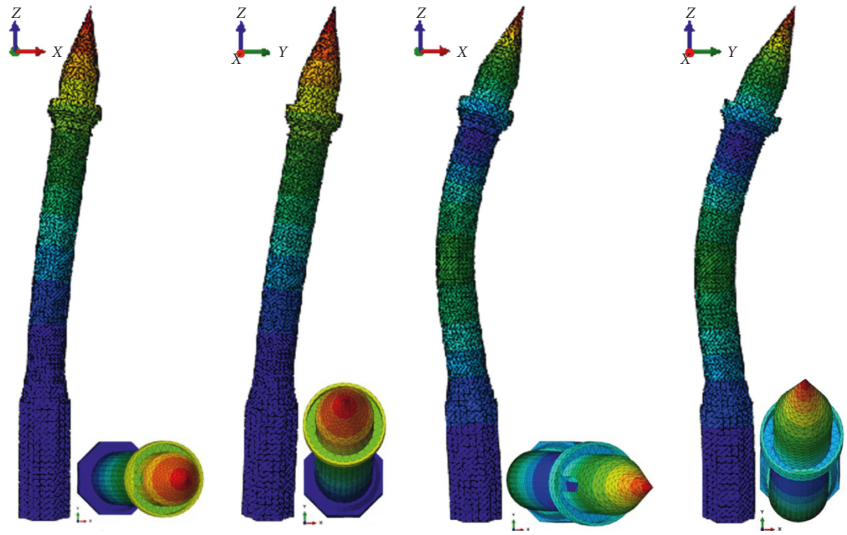

Figure 4: The first four mode shapes profile and plan views and frequency values from the initial finite element model. (a) Mode 1: freq. = 0.849 (cycles/time); (b) Mode 2: freq. = 0.851 (cycles/time); (c) Mode 3: freq. = 4.339 (cycles/time); (d) Mode 4: freq. = 4.364 (cycles/time).

Figure 5: Locations and directions of the accelerometers on the minaret.

The tension damage effects calculated by CDP analysis at the end of the analysis are presented in Figure 18. The tension damage on masonry of the minaret begins at 13.52 s, and the plastic deformation value reaches 0.014 at the end of the analysis (t = 25 s) (Figure 19). Only small number of elements exceeds the value of 0.0002 which is the critical damage strain value (Figure 9). Damage parameters remain around 70% of the tensile and pressure. It is envisaged that the minaret would overcome this earthquake with minor damage. It can be generally said that the masonry minaret is safe under the Çay-Sultandağı earthquake.

2.7.2. Dinar Earthquake. Nonlinear time-history analysis of the minaret under the Dinar earthquake shows that the maximum lateral displacement values are 17.4 cm and 27.8 cm in $U1$ and $U2$ directions, respectively (Figure 20).

Critical maximum and minimum principle stress contours under the Dinar earthquake are presented in Figure 21. The compression damage percentages of the minaret at the end of the analysis are presented in Figure 22.

The compression damage on masonry of the minaret begins at 3.8 s, and the plastic deformation value reaches 0.17 at the end of the analysis (Figure 23). Only small number of elements exceeds the value of 0.004 which is the critical damage strain value (Figure 9).

The tension damage effects calculated by CDP analysis at different time steps are presented in Figure 24. The tension damage on masonry of the minaret begins at 3.3 s, and the plastic deformation value reaches 0.38 at the end of the analysis (t = 25 s) (Figure 25). The upper part of the transition segment exceeds the value of 0.0002 which is the critical damage strain value (Figure 9). Damage parameters are around 85% of the tension and 90% of the pressure. It is thought that the minaret will face major damage and failure in this earthquake hazard. The events observed have shown that thin and tall masonry structures like minarets are damaged particularly at the transition segments [37].

The locations of compression and tension regions under linear and nonlinear time-history analysis are coincided. Since the masonry cannot recover tensile stress, the observed tension regions are critical although these regions are limited. Under a high ground motion, the minaret may be considerably damaged from these regions, and a special precaution must be implemented to these regions.

3. Conclusions

Historical structures are of great importance to a country. The historical roots of a country have been exhibited by them. Therefore, they must be passed on from generation to generation. This study includes a valuable contribution to this goal. Seismic damage propagation estimations in the

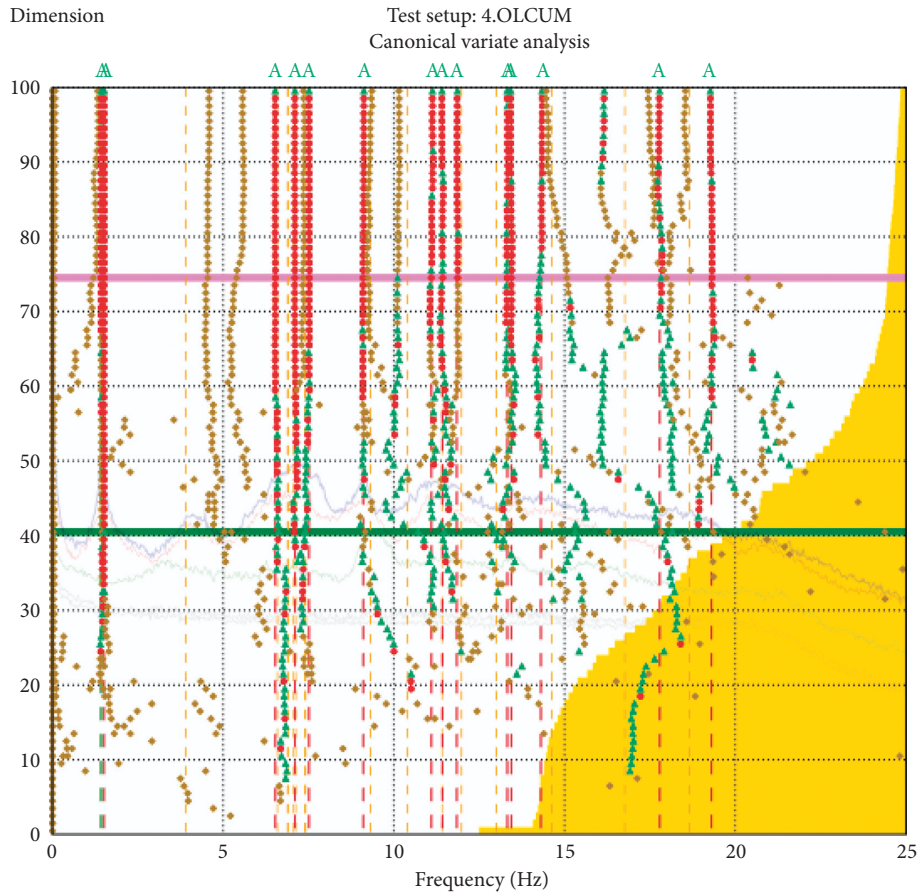

Figure 6: Stabilization diagram of estimated state space models obtained from the SSI technique.

Table 4: The experimental dynamic characteristics.

Mod	1	2	3	4
Frequencies (Hz)	1.425	1.516	6.530	7.108

Table 5: The dynamic characteristics obtained before and after the FEM calibration.

Mode	Numerical frequencies FEM (Hz)		Experimental frequencies OMA	Difference (%)	
	Before update	After update	SSI	Before update	After update
1	0.849	1.425	1.425	−57	0.00
2	0.851	1.531	1.516	−66	0.15
3	4.339	6.548	6.530	22	0.18
4	4.362	6.692	7.108	27	−4.16

historical clay brick masonry minaret under different ground motion levels by using the updated FEM are implemented in this paper. Dinar (1995) and Çay-Sultandağı (2002) earthquakes are considered in the linear and nonlinear time-history analyses. It is seen that only the material information made by material tests is not sufficient. The structure must be fully investigated. After the OMA experiment, as a result of the finite element solution improvement, the modulus of elasticity increased from 1300 MPa to 5200 MPa. In the first mode, the natural frequency increased from 0.849 to 1.425. Mode shapes are in parallel with those in the experimental study. A three-dimensional finite element model of the minaret is calibrated using the ambient vibration test results. The difference between the experimental and numerical frequencies, at the first 4 modes, is about 43% before the model calibration and 1.12% after the calibration. Due to their intensity, the results from the Dinar earthquake are bigger than those from the Çay-Sultandağı earthquake. When the two earthquakes are compared, the end point of the minaret is 5 cm in the Çay-Sultandağı earthquake and 38 cm in the Dinar earthquake. Approximately 8 times the displacement difference is observed. The minaret has a displacement difference of 8 times. Approximately 6 times a stress difference occurred. Under the Çay-Sultandağı earthquake, damage parameters remain around 70% of the tensile and pressure. It is thought that the minaret will overcome this earthquake with minor damage. It can be generally said that the masonry minaret is safe under the Çay-Sultandağı earthquake. Under the Dinar earthquake, damage parameters are around 85% of the tension and 90% of the pressure. It is thought that the minaret would face major damage and failure in this earthquake hazard.

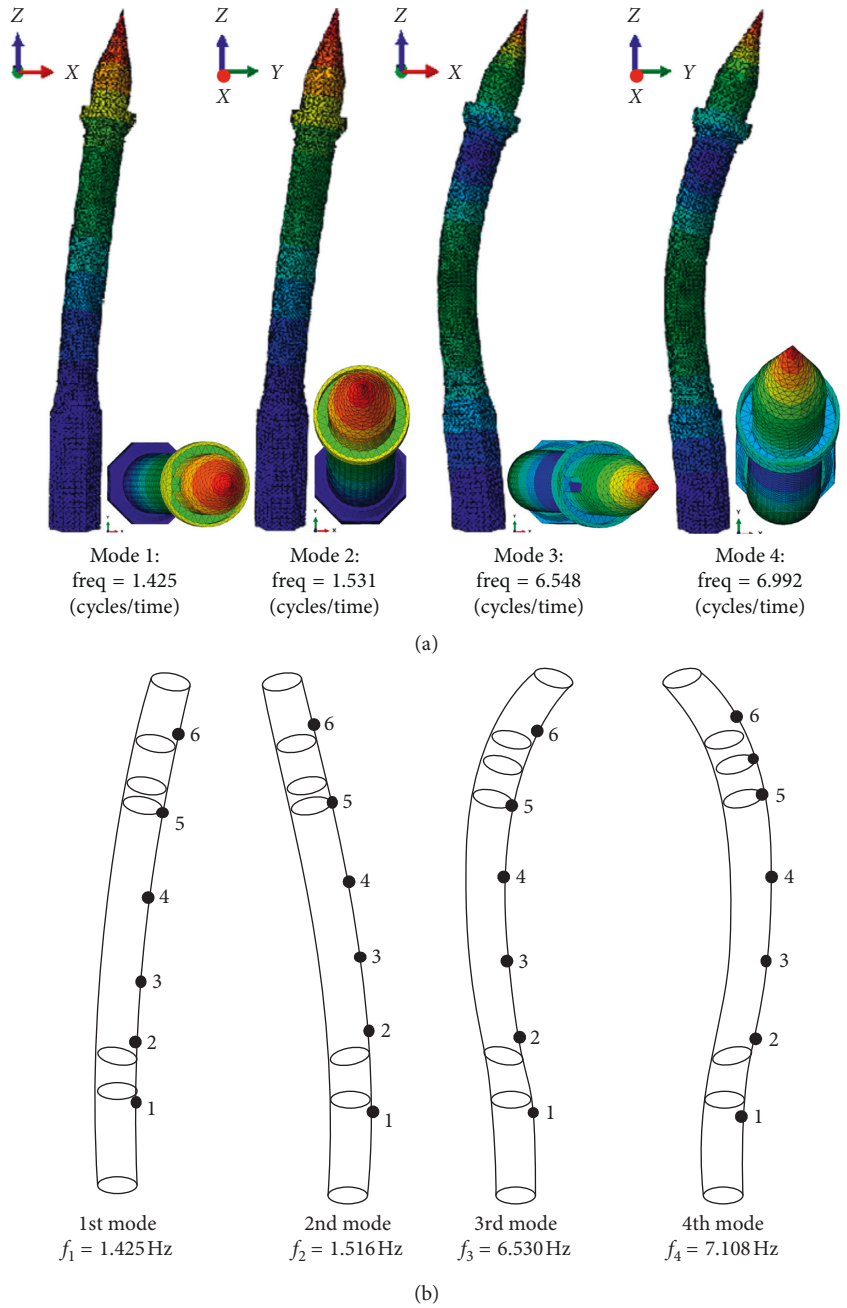

Figure 7: The first four calibrated and experimental mode shapes. (a) Updated FEM mode shapes profile and plan views. (b) Experimental mode shapes profile and plan views.

Table 6: Material parameters for masonry in the CDP model.

Dilation angle	Eccentricity	σ_{bo}/σ_{co}	K
100	0.1	1.16	0.666

The Çay-Sultandağı earthquake would inflict limited damage on the minaret, whereas the Dinar earthquake would damage some parts of the elements in the transition segment of the minaret. It is observed that linear time-history analysis results do not reflect actual response of the clay brick masonry minaret during the earthquake. The maximum and minimum principal stresses obtained from the nonlinear analyses exceeded the tensile and compressive strength values of the masonry, and they concentrated on the transition region. At the end of the study, the damage of the historical minaret against the two selected earthquakes was obtained, and it was determined that the minaret was at risk of collapse during a severe earthquake.

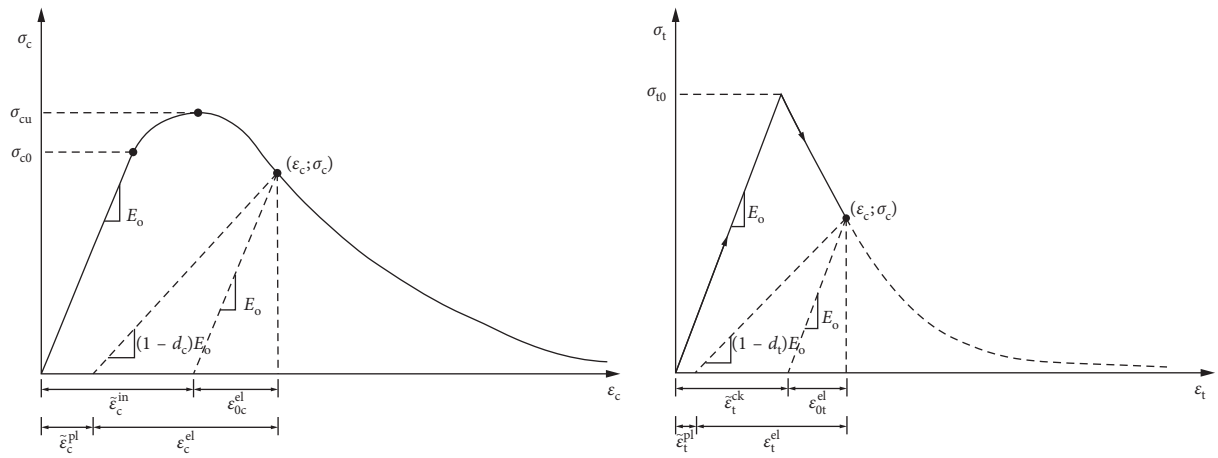

Figure 8: Damage plasticity stress-strain diagrams: (a) uniaxial tension and (b) uniaxial compression.

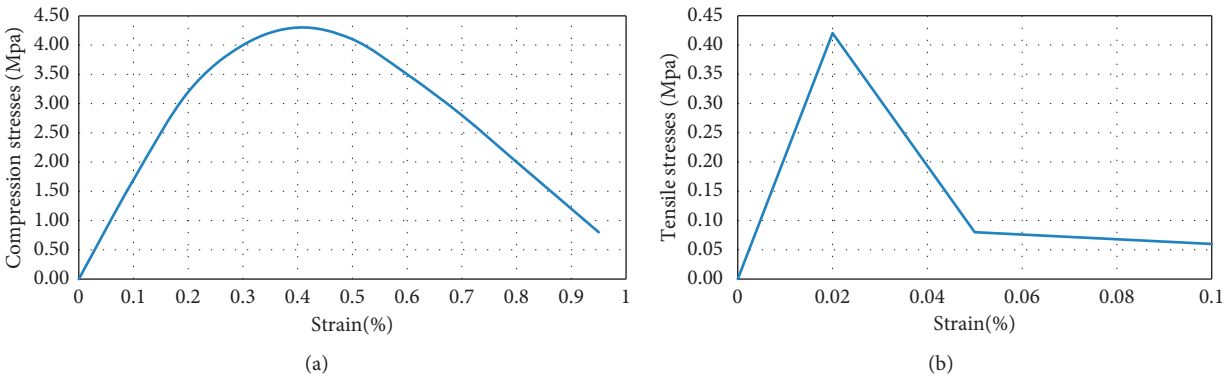

Figure 9: Stress-strain relationship for brick masonry. (a) Compression. (b) Tension.

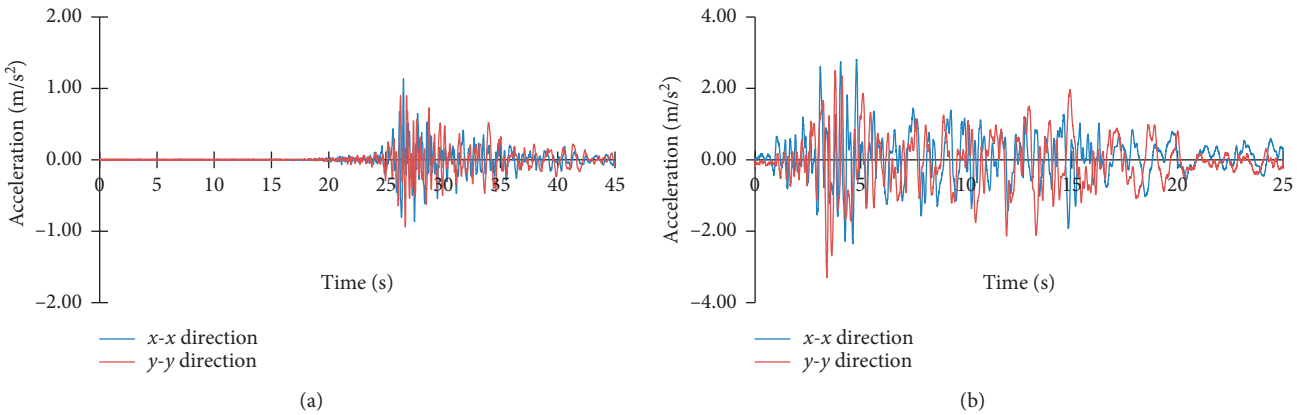

Figure 10: (a) Çay-Sultandağı and (b) Dinar earthquake acceleration records.

It can be seen from the past earthquakes that masonry minarets are damaged particularly at the transition segments. Besides, occurrence of stress concentration in the regions where section variations take place indicates that the calibrated finite element model represents the behavior of the minaret as close to reality as possible. Therefore, safety

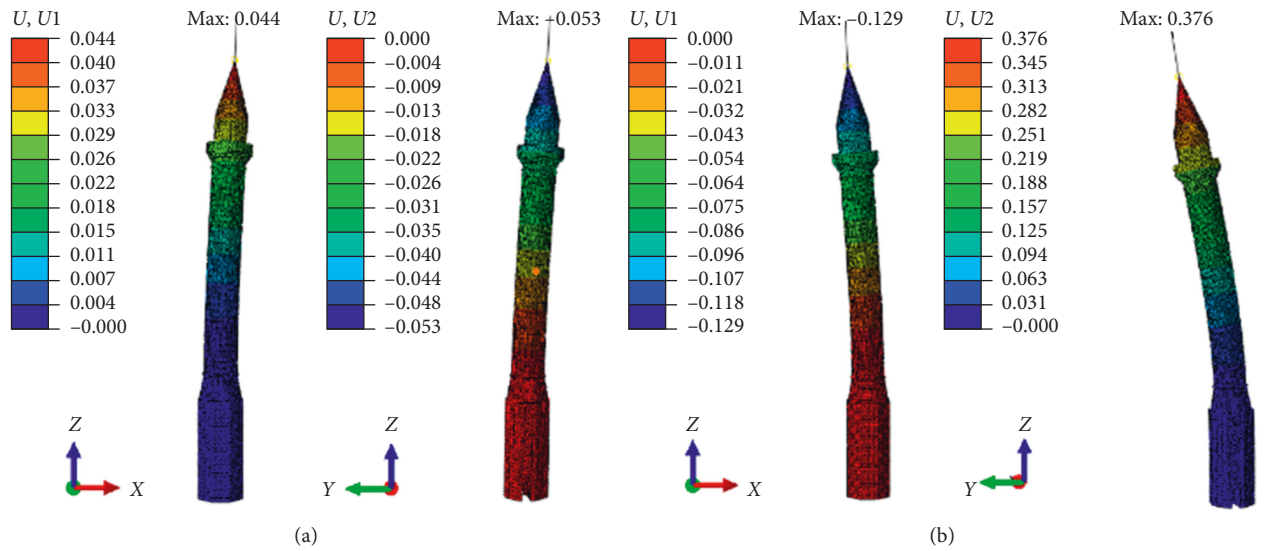

Figure 11: Maximum displacement contour shapes under the earthquakes. (a) Çay-Sultandağı earthquake. (b) Dinar earthquake.

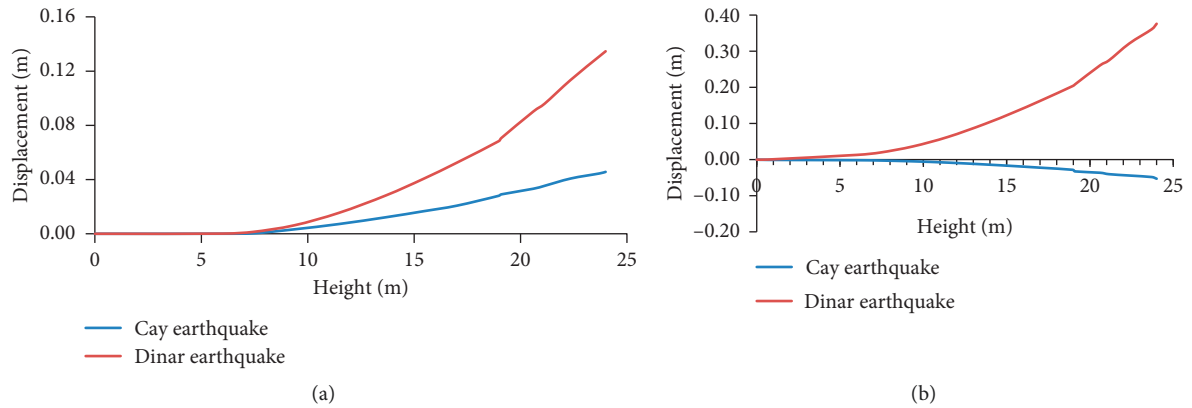

Figure 12: Lateral displacements throughout the height for the linear analyses. (a) $U1$. (b) $U2$.

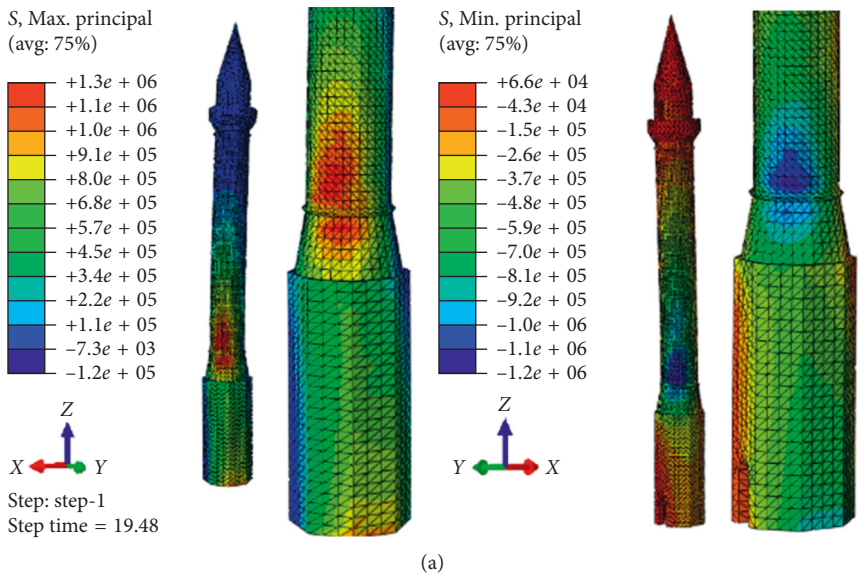

Figure 13: Continued.

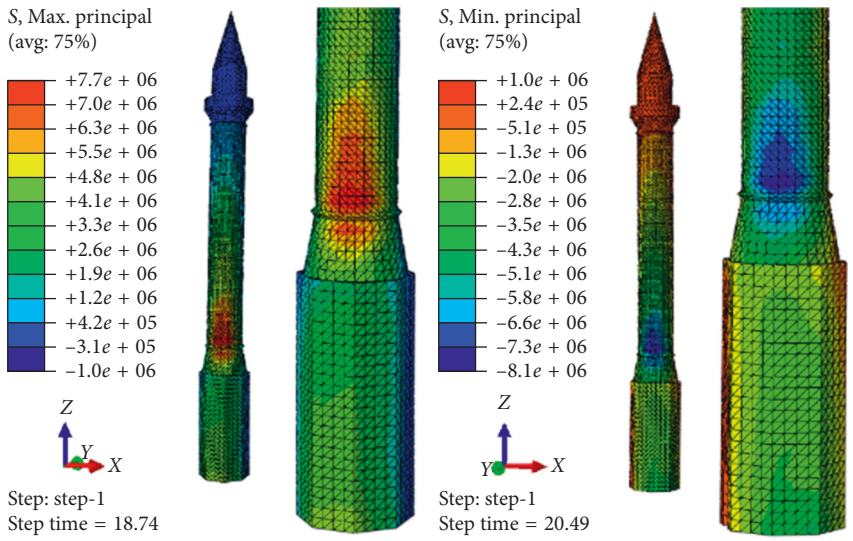

(b)

Figure 13: Maximum and minimum principal stresses contour under the earthquakes. (a) Çay-Sultandağı earthquake. (b) Dinar earthquake.

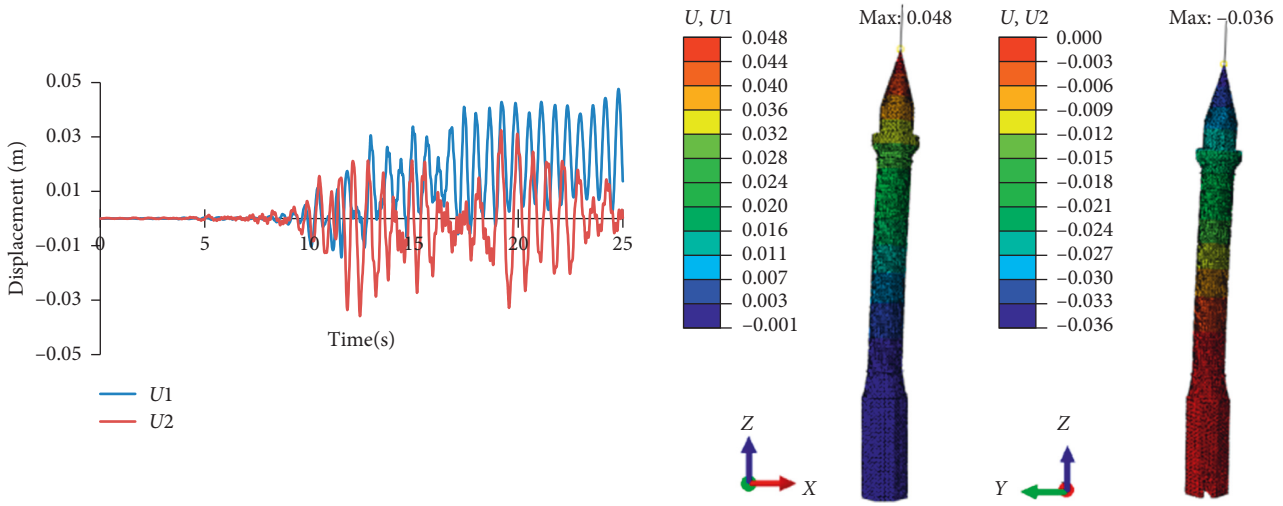

Figure 14: Time-history and contour graphs of displacements in the minaret under the Çay-Sultandağı earthquake.

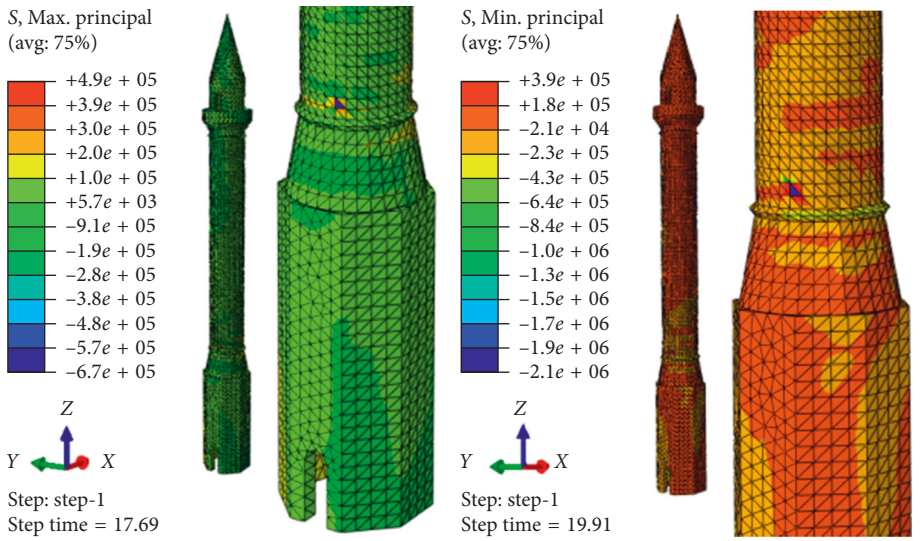

Figure 15: Maximum and minimum principal stresses in the minaret under the Çay-Sultandağı earthquake.

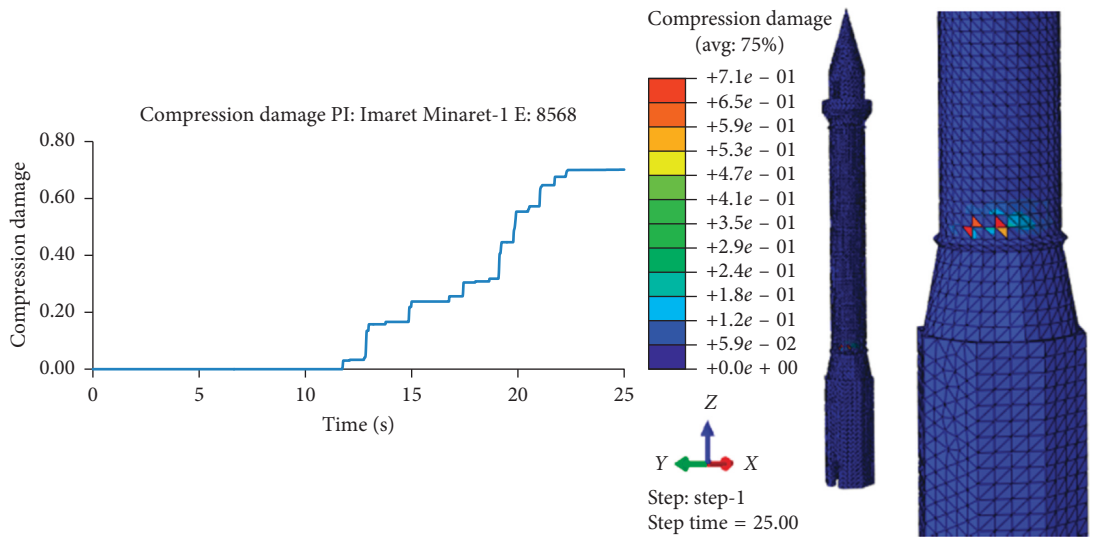

Figure 16: Compression damage distribution for the minaret at different time steps under the Çay-Sultandağı earthquake.

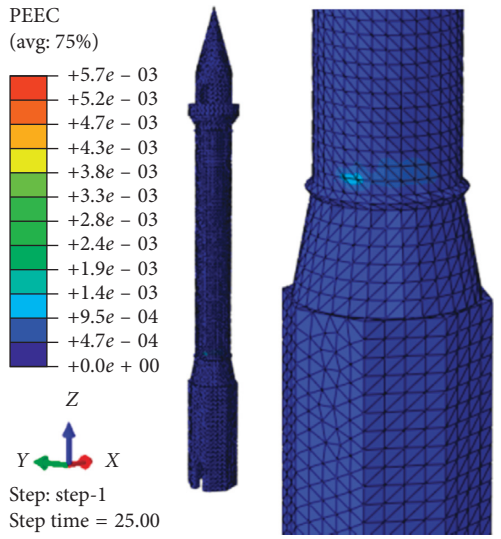

Figure 17: Compressive plastic strain contour under the Çay-Sultandağı earthquake.

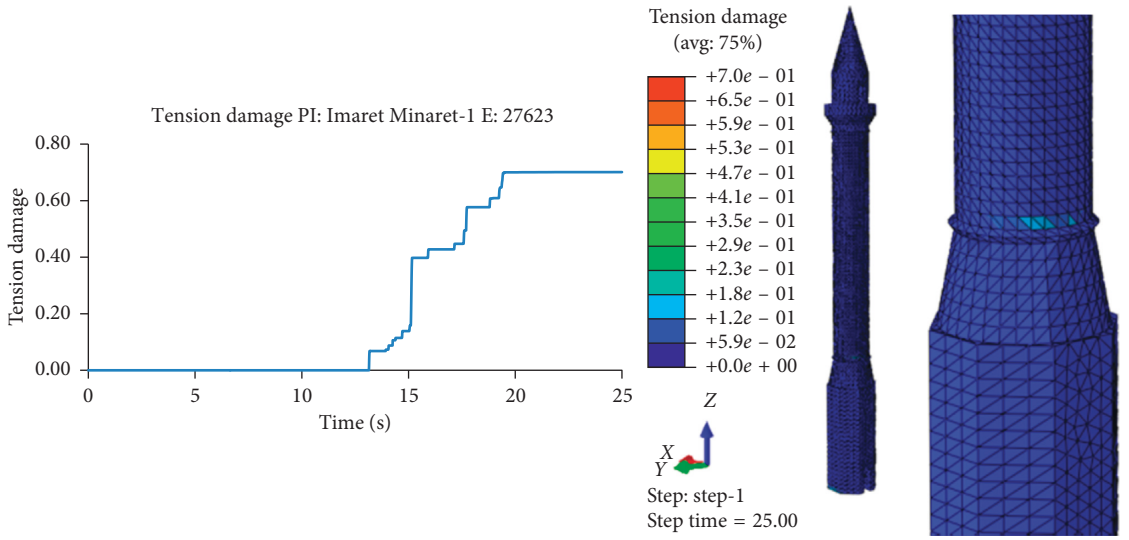

Figure 18: Tension damage distribution for the minaret at different time steps under the Çay-Sultandağı earthquake.

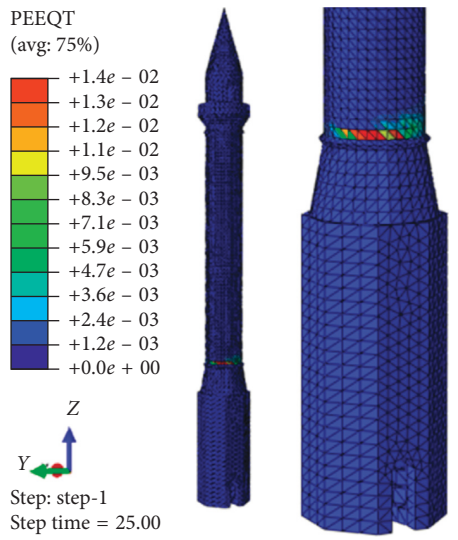

Figure 19: Tension plastic strain contour under the Çay-Sultandağı earthquake.

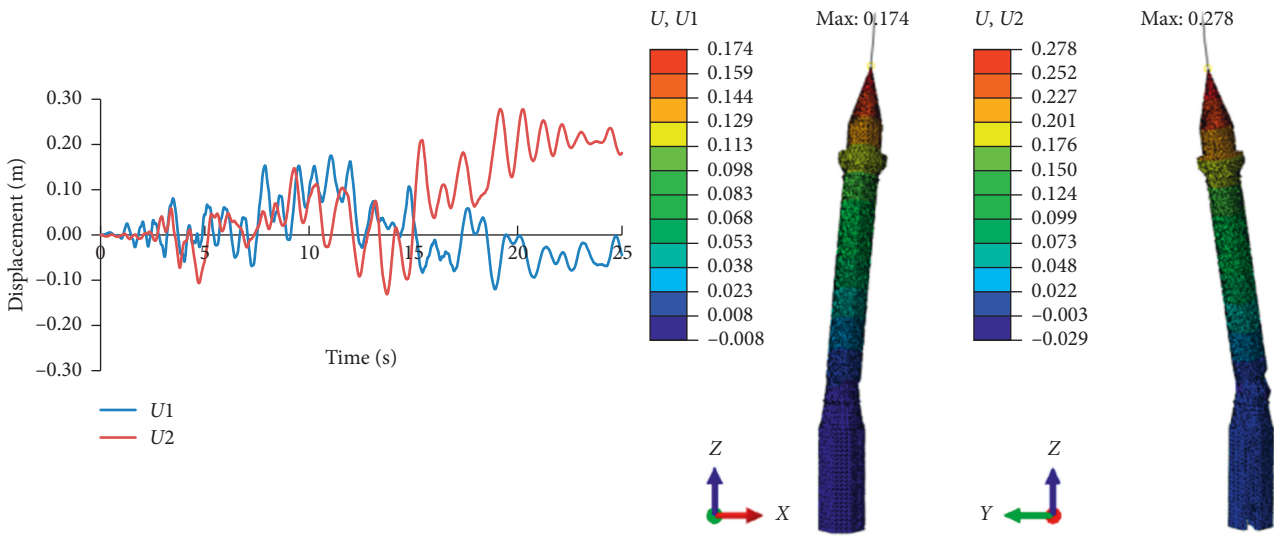

Figure 20: Time-history and contour graphs of displacements in the minaret under the Dinar earthquake.

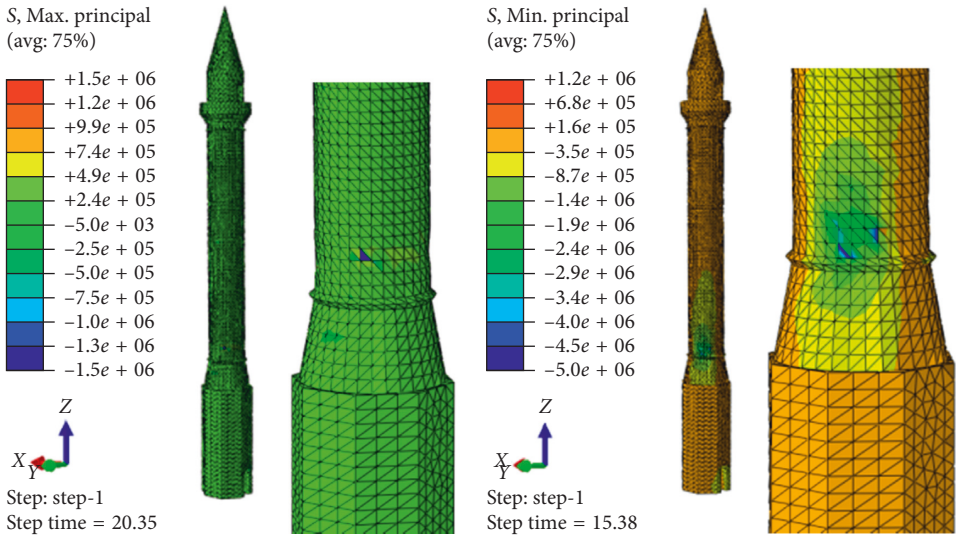

Figure 21: Maximum and minimum principal stresses in the minaret under the Dinar earthquake.

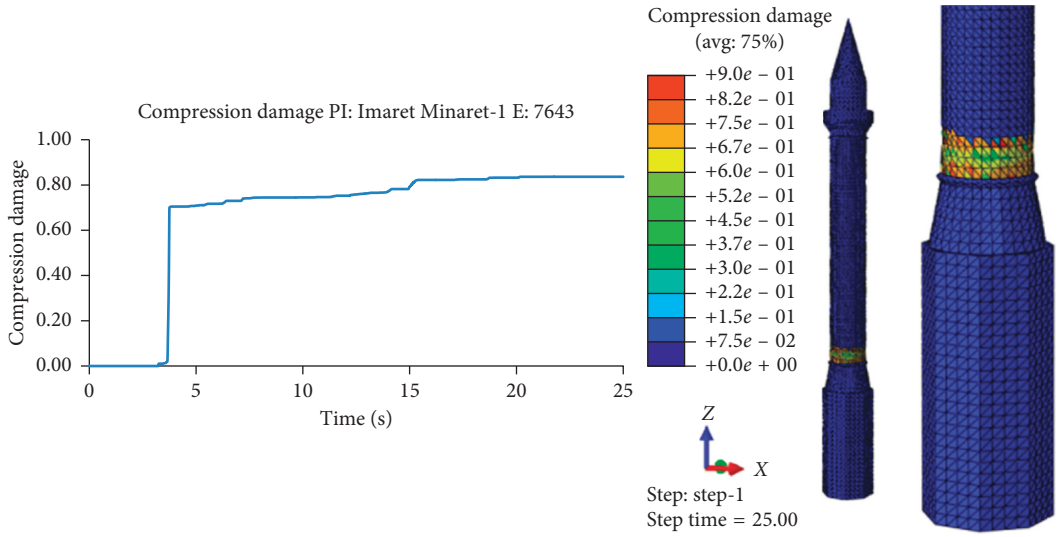

Figure 22: Compression damage distribution for the minaret at different time steps under the Dinar earthquake.

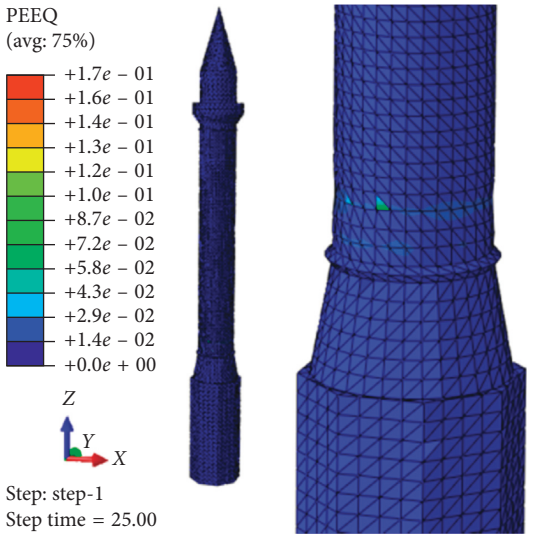

Figure 23: Compressive plastic strain contour under the Dinar earthquake.

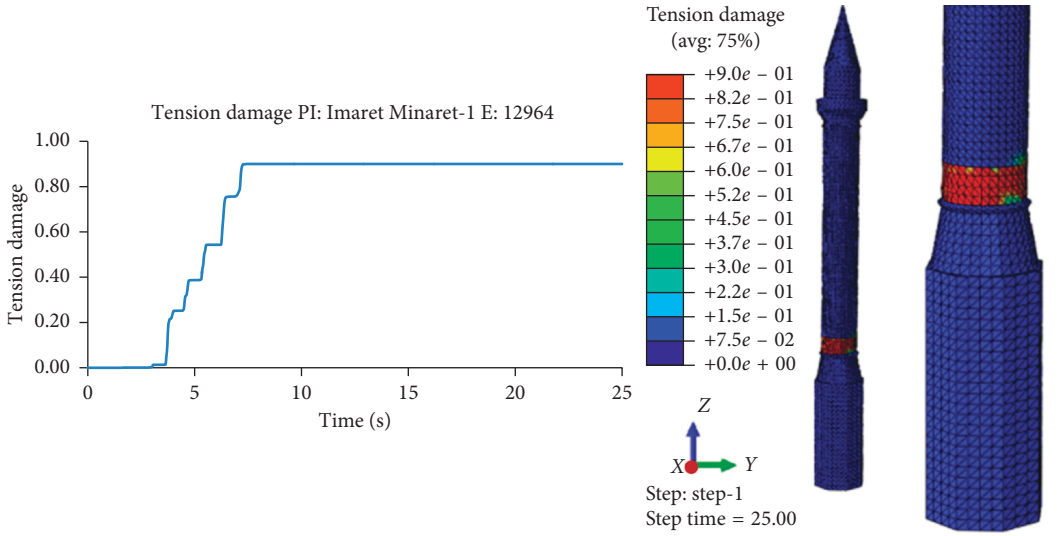

Figure 24: Tension damage distribution for the minaret at different time steps under the Dinar earthquake.

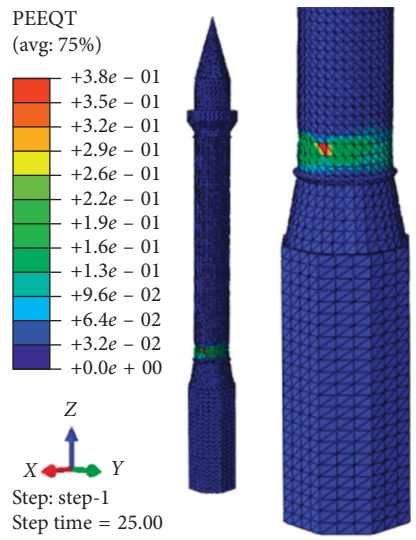

Figure 25: Tension plastic strain contour under the Dinar earthquake.

assessment of the masonry minarets under earthquakes should be evaluated considering calibrated finite element models and nonlinear time-history analyses.

Data Availability

Readers can access the earthquake accelerations data. The earthquake accelerations data used to support the findings of this study have been deposited in the repository available at http://kyhdata.deprem.gov.tr/2K/kyhdata_v4.php?dst=TU9EVUxFX05BTUU9ZXZ0RmlsZSZNT0RVTEVfVEFTSz1zZWFyY2g%3D.

Conflicts of Interest

The author declares that there are no conflicts of interest regarding the publication of this paper.

Acknowledgments

This research was conducted using the facilities of Manisa Celal Bayar University.

References

[1] F. Cakir, B. S. Seker, A. Durmus, A. Dogangun, and H. Uysal, "Seismic assessment of a historical masonry mosque by experimental tests and finite element analyses," *KSCE Journal of Civil Engineering*, vol. 19, no. 1, pp. 158–164, 2014.

[2] A. Bayraktar, B. Sevim, A. C. Altunişik, and T. Türker, "Earthquake analysis of reinorced concrete minarets using ambient vibration test results," *The Structural Design of Tall and Special Buildings*, vol. 19, 2008.

[3] G. M. Binda, R. Tongini Folli, and G. M. Roberti, "Survey and inevstigation for the diagnosis of damaged masonry structures: the "Torrazzo" of Cremona," in *Proceedings of 12th International Brick/Block Masonry Conference*, Madrid, Spain, June 2000.

[4] S. Atamturktur, P. Fanning, and T. E. Boothby, "Traditional and operational modal testing of masonry vaults," *Proceedings of the Institution of Civil Engineers-Engineering and Computational Mechanics*, vol. 163, no. 3, pp. 213–223, 2010.

[5] A. Bayraktar, A. C. Altunişik, B. Sevim, and T. Türker, "Seismic response of a historical masonry minaret using a finite element model updated with operational modal testing," *Journal of Vibration and Control*, vol. 17, no. 1, pp. 129–149, 2010.

[6] C. Gentile and A. Saisi, "Ambient vibration testing of historic masonry towers for structural identification and damage assessment," *Construction and Building Materials*, vol. 21, no. 6, pp. 1311–1321, 2007.

[7] F. J. Pallarés, A. Agüero, and S. Ivorra, "A comparison of different failure criteria in a numerical seismic assessment of an industrial brickwork chimney," *Materials and Structures/Materiaux et Constructions*, vol. 42, no. 2, pp. 213–226, 2008.

[8] A. Tomaszewska and C. Szymczak, "Identification of the Vistula Mounting tower model using measured modal data," *Engineering Structures*, vol. 42, pp. 342–348, 2012.

[9] D. Foti, M. Diaferio, N. I. Giannoccaro, and M. Mongelli, "Ambient vibration testing, dynamic identification and model updating of a historic tower," *NDT & E International*, vol. 47, pp. 88–95, 2012.

[10] A. Mortezaei, A. Kheyroddin, and H. R. Ronagh, "Finite element analysis and seismic rehabilitation of a 1000-year-old heritage listed tall masonry mosque," *The Structural Design of Tall and Special Buildings*, vol. 21, no. 5, pp. 334–353, 2010.

[11] A. D'Ambrisi, V. Mariani, and M. Mezzi, "Seismic assessment of a historical masonry tower with nonlinear static and dynamic analyses tuned on ambient vibration tests," *Engineering Structures*, vol. 36, pp. 210–219, 2012.

[12] G. Bartoli, M. Betti, and S. Giordano, "In situ static and dynamic investigations on the "Torre Grossa" masonry tower," *Engineering Structures*, vol. 52, pp. 718–733, 2013.

[13] F. Minghini, G. Milani, and A. Tralli, "Seismic risk assessment of a 50m high masonry chimney using advanced analysis techniques," *Engineering Structures*, vol. 69, pp. 255–270, 2014.

[14] M. Diaferio, D. Foti, and N. I. Giannocaro, "Non-destructive characterization and identification of the modal parameters of an old masonry tower," in *Proceedings of 2014 IEEE Workshop on Environmental, Energy and Structural Monitoring Systems Proceedings (EESMS 2014)*, pp. 57–62, Naples, Italy, September 2014.

[15] M. Diaferio, D. Foti, C. Gentile, N. I. Giannoccaro, and A. Saisi, "Dynamic testing of a historical slender building using accelerometers and radar," in *Proceedings of 6th International Operational Modal Analysis Conference (IOMAC 2015)*, Gijon, Spain, May 2015.

[16] A. Preciado, "Seismic vulnerability and failure modes simulation of ancient masonry towers by validated virtual finite element models," *Engineering Failure Analysis*, vol. 57, pp. 72–87, 2015.

[17] A. Preciado, S. T. Sperbeck, and A. Ramírez-Gaytán, "Seismic vulnerability enhancement of medieval and masonry bell towers externally prestressed with unbonded smart tendons," *Engineering Structures*, vol. 122, pp. 50–61, 2016.

[18] M. Hejazi, S. M. Moayedian, and M. Daei, "Structural analysis of Persian historical brick masonry minarets," *Journal of Performance of Constructed Facilities*, vol. 30, no. 2, article 04015009, 2016.

[19] A. Demir, H. Nohutcu, E. Ercan, E. Hokelekli, and G. Altintas, "Effect of model calibration on seismic behaviour of a historical mosque," *Structural Engineering and Mechanics*, vol. 60, no. 5, pp. 749–760, 2016.

[20] R. Livaoğlu, M. H. Baştürk, A. Doğangün, and C. Serhatoğlu, "Effect of geometric properties on dynamic behavior of historic masonry minaret," *KSCE Journal of Civil Engineering*, vol. 20, no. 6, pp. 2392–2402, 2016.

[21] T. Kocaturk and Y. S. Erdogan, "Earthquake behavior of M1 minaret of historical sultan ahmed mosque (blue mosque)," *Structural Engineering and Mechanics*, vol. 59, no. 3, pp. 539–558, 2016.

[22] S. Ivorra, V. Brotóns, D. Foti, and M. Diaferio, "A preliminary approach of dynamic identification of slender buildings by neuronal networks," *International Journal of Non-Linear Mechanics*, vol. 80, pp. 183–189, 2016.

[23] M. Shakya, H. Varum, R. Vicente, and A. Costa, "Empirical formulation for estimating the fundamental frequency of slender masonry structures," *International Journal of Architectural Heritage*, vol. 10, no. 1, pp. 55–66, 2014.

[24] G. Castellazzi, A. M. D'Altri, S. de Miranda, and F. Ubertini, "An innovative numerical modeling strategy for the structural analysis of historical monumental buildings," *Engineering Structures*, vol. 132, pp. 229–248, 2017.

[25] M. Diaferio, D. Foti, N. I. Giannoccaro, and S. Ivorra, "Optimal model through identified frequencies of a masonry building structure with wooden floors," *International Journal of Mechanics*, vol. 8, no. 1, pp. 282–288, 2014.

[26] D. Foti, M. Diaferio, N. I. Giannoccaro, and S. Ivorra, "Structural identification and numerical models for slender historical structures," in *Handbook of Research on Seismic Assessment and Rehabilitation of Historic Structures, Chapter 23*, P. Asteris and V. Plevris, Eds., pp. 674–703, Engineering Science Reference, Hershey, PA, USA, 2015.

[27] Dassault Systèmes Simulia Corp., *ABAQUS V10*, Dassault Systèmes Simulia Corp., RI, USA, 2010.

[28] H. Nohutcu, A. Demir, E. Ercan, E. Hokelekli, and G. Altintas, "Investigation of a historic masonry structure by numerical and operational modal analyses," *The Structural Design of Tall and Special Buildings*, vol. 24, no. 13, pp. 821–834, 2015.

[29] European Committee for Standardization, *Eurocode 6*, European Committee for Standardization, Brussels, Belgium, 1996.

[30] P. B. Lourenço, "Assessment of the stability conditions of a Cistercian cloister," in *Proceedings of 2nd International Congress on Studies in Ancient Structures*, Istanbul, Turkey, July 2001.

[31] A. Koçak, *Linear and nonlinear static and dynamic analysis of historical masonry structures: Küçük Aya Sofya Mosque*, Ph.D. Thesis, Yıldız Technical University, Institute of Science and Technology, Civil Engineering Department, İstanbul, Turkey, 1999.

[32] Testlab-Network, *Computer Program*, TDG, Turkey, 2012.

[33] ARTeMISModal Pro 3.0, 2014, http://www.svibs.com.

[34] P. Van Overschee and B. De Moor, *Subspace Identification for Linear Systems*, Kluwer Academic Publishers, Dordrecht, Netherlands, 1996.

[35] B. Peeters, *System Identification and Damage Detection in Civil Engineering*, 2000, https://lirias.kuleuven.be/handle/123456789/212304.

[36] H. B. Kaushik, D. C. Rai, and S. K. Jain, "Stress-strain characteristics of clay brick masonry under uniaxial compression," *Journal of Materials in Civil Engineering*, vol. 19, no. 9, pp. 728–739, 2007.

[37] A. Bayraktar, A. C. Altunişik, and M. Muvafik, "Damages of minarets during Erciş and Edremit earthquakes, 2011 in Turkey," *Smart Structures and Systems*, vol. 14, no. 3, pp. 479–499, 2014.